

Tension and Compression Optimization of Integrated Loop Technology Joint

B. Kropík^{1,*}, T. Ponížil², A. Malá¹, T. Zámečníková¹,

N. Schmidová¹, K. Doubrava¹, M. Dvořák¹, H. Chlup¹, T. Mareš¹

¹ *Department of Mechanics, Biomechanics and Mechatronics, Faculty of Mechanical Engineering, Czech Technical University in Prague. Technická 4, 160 00 Prague 6, Czech Republic*

² *Compo Tech PLUS, spol. s r. o., Nová 1316, 342 01 Sušice, Czech Republic*

* *bohupil.kropik@fs.cvut.cz*

Abstract: This contribution deals with the experimental part of development of an integrated loop technology joint from first idea to improved design of joint according to tension and compression tensile test. Paper is focused on the experimental part of development with support of FEM analysis outputs. Initial experiments and simulations led to the change of production technology of integrated loop technology joints. Then different variants of new specimens were made by change of section layers positions to achieve the highest tension and compression strength. These new specimens were subjected to detailed experimental investigation with use of digital image correlation, acoustic emission, strain measurement and video recording and the optimal variant was found. Final variant was subjected to additional tests in other loading scenarios which will be published separately.

Keywords: optimization; CFRP; integrated joint; filament winding; integrated loop technology.

1 Introduction

Current situation in the field of joining techniques of composites (whether with other materials or with each other) is still poorly dependent on automation. Most widely expanded connection techniques of composites, such as manual lamination or bonding, are highly dependent on human work, which also affects the quality and repeatability of these joints. There are some automated techniques such as wound pin joints of metal inserts in composite tubes, but this is hard to achieve with composite to composite joint without any additional inserts. At this point it is the turn of the Integrated Loop Technology (ILT) joint which allows the connection of composite tubes to any other tube with possibility of automated production. Members of our team have been working on this for a long time. More complex view on Finite Element Method (FEM) analysis of the first generation of specimens with ILT joints is shown in reference [1]. First generation of specimens with ILT joints is discussed in reference [2]. As a demonstration of application could be shown the bicycle frame main triangle of mountain bicycle used for enduro races presented last year in reference [3] which was made with use of ILT joints. Some basic measurements of the first generation of specimens using Acoustic Emission (AE) are discussed in reference [4]. Filament wound tube samples made of carbon fibers with the ILT joints were optimized according to the analysis and experiment in the form of tensile and compressive tests. Specimens were monitored with a wide range of monitoring methods such as Digital Image Correlation (DIC), AE, Strain measurement and video monitoring during the experimental part of optimization to identify their behavior and failures.

2 Second generation of specimens

According to the results of experiments of first generation of specimens a change was made in the technology of production process of ILT joints to avoid the fiber-free area near the joint. Technology was adjusted by

moving of the pins, so the winding of tube was ended behind the problematic area. New specimen is shown in the Fig. 1.



Fig. 1: New specimen with ILT joint.

New set of specimens was made by variation of fiber areas shown in Fig. 2 and Fig. 3. The relevant part of area is always highlighted in red. Overview of specimen variants is in Tab. 1. Used fiber areas are as follows:

- SN (“XY”) – the area of fibers forming the main part of the tube. The “XY” represents number in brackets which means the \pm angle of laid fibers to the longitudinal axis of tube. This area is shown in Fig. 2a.
- A “X” – the area of fibers forming the ILT joint. The “X” represents number and means that these fibers are wrapped around the joined tube (1) or not (2). These fibers are laid on the sides and oriented at angle of 0° . These areas are shown in Fig. 2b and Fig. 3b.
- Hoop – the area of fibers forming the main part of the tube oriented at angle of nearly 90° . This area is shown in Fig. 3a.

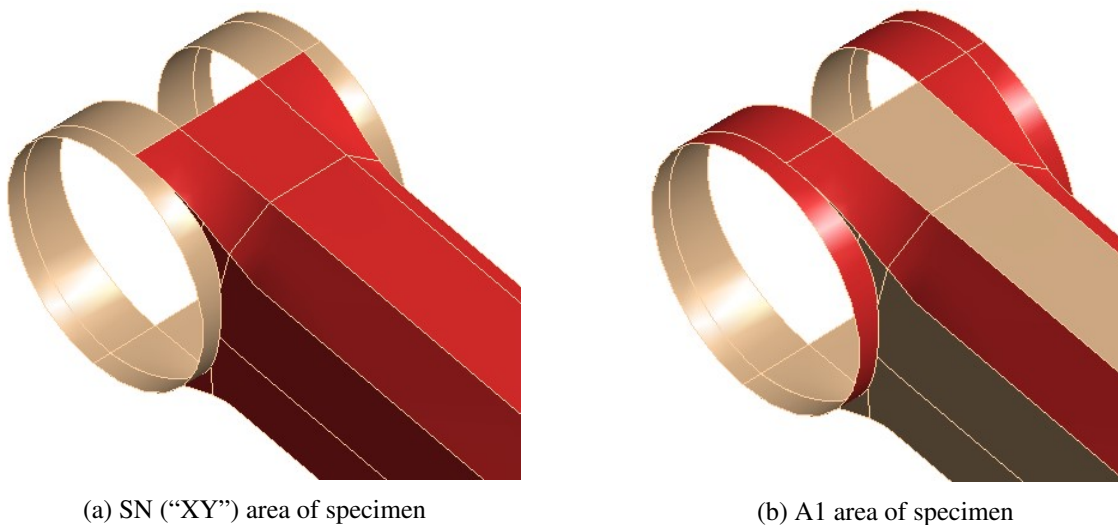


Fig. 2: Fiber area types of new specimens.

In addition to change in production technology, the section A1 with wrapped fibers around the joined tube and the usage of composite tube as joined part are major changes between generations of specimens. All specimens consist of five layers which are chosen from these four described areas.

Tab. 1: Overview of new specimens and their composition.

Specimen type	First layer	Second layer	Third layer	Fourth layer	Fifth layer
SN_02	SN (45)	A2	Hoop	SN (0)	SN (45)
SN_07	Hoop	A1	SN (45)	SN (0)	SN (45)
SN_08	Hoop	A2	SN (45)	SN (0)	SN (45)
SN_09	Hoop	A1	A1	SN (45)	SN (45)

Due to the amount of new specimen variants, the time-consuming nature of specimen production and costs,

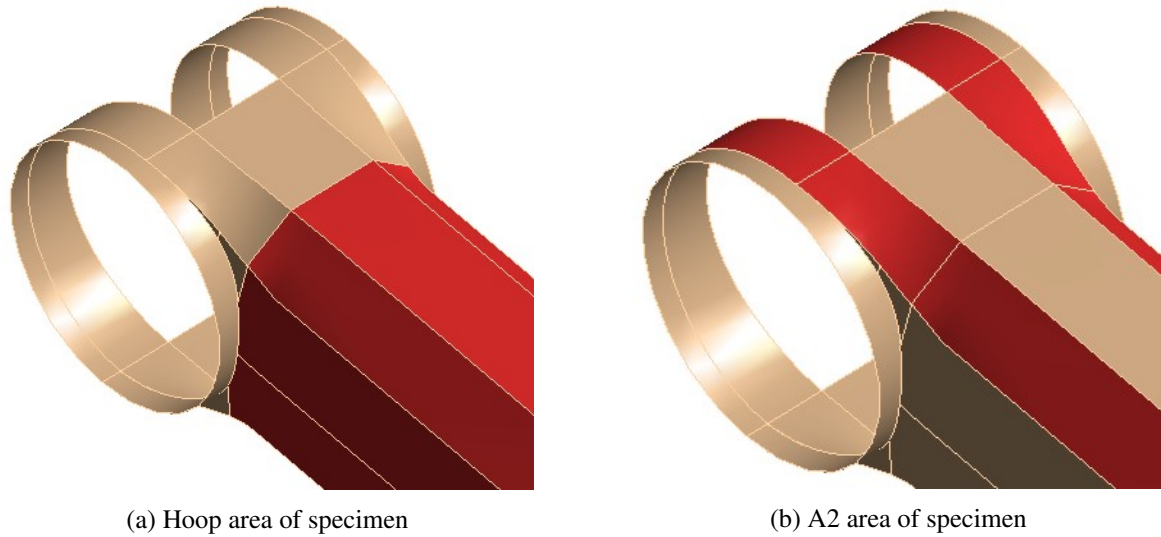


Fig. 3: Fiber area types of new specimens.

a detailed FEM analysis was performed first. Based on the analysis, specimen types SN_02, SN_07 and SN_08 were chosen for more detailed analysis and tensile test. Specimen SN_09 was designed later based on the requirement of simpler production and according to obtained experimental results and it was also subjected to detail analysis and tensile test. Chosen specimens allow us to experimentally assess the influence of wrapping of fibers around tube in A section and to compare influence of swapping the fiber areas.

3 Experimental procedure

Chosen specimens were subjected to the tensile and compressive test using electromechanical universal loading machine TIRA test 2300. Number of specimens, according to the individual variants and loading scenario, are given in Tab. 2. Based on results of first generation of specimens, it was necessary to verify that the fiber-free area near the joint is not affecting the strength of designed joint anymore. Therefore, two specimens were selected in each variant and loading scenario for Digital Image Correlation (DIC) method monitoring. The specimens were also equipped with 1-axis linear strain gauge which was used for comparison of specimens and optimization of FEM analysis model. Mechanical loading of all specimens was recorded also on camera and monitored by AE method. All specimens were loaded with displacement at loading rate of 2 mm/min. All measured forces presented below are related to the maximal tension force achieved during experiments and all mechanical strains are related to the maximal tension strain recorded during experiments given as normalized strain.

Tab. 2: Number of chosen specimens divided according to different types of loading scenarios.

Specimen type	Tension	Compression
SN_02	2	3
SN_07	2	4
SN_08	2	4
SN_09	2	2

3.1 DIC method

Configuration of DIC method setup was chosen based on previous experiences as 3D with two cameras capturing the same area of specimen as close to the ILT joint as the measured assembly allows. Configuration is shown in Fig. 4.

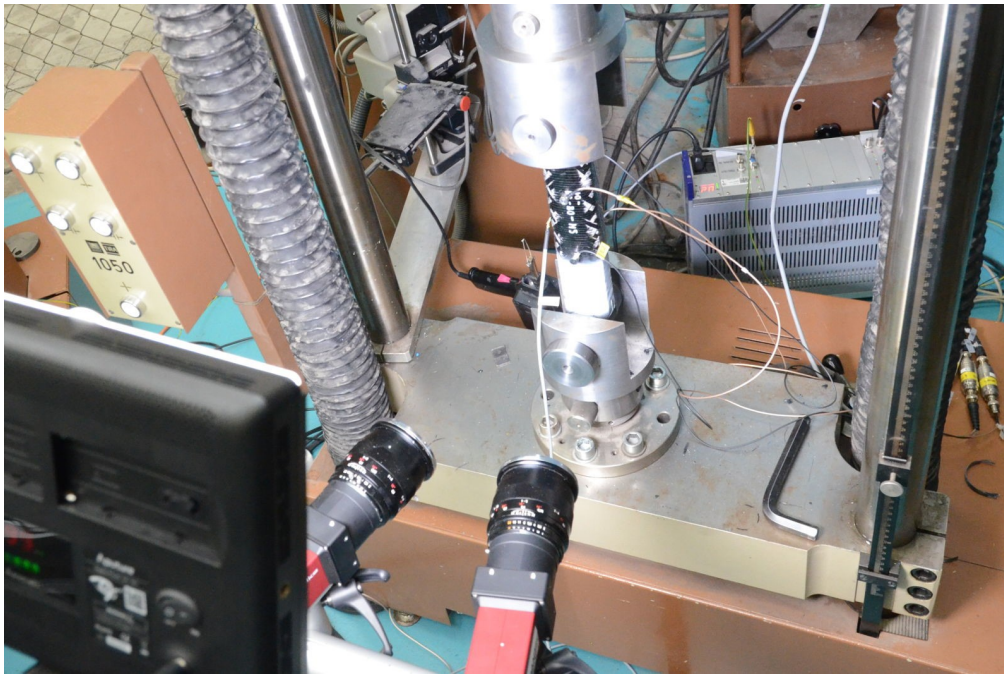


Fig. 4: Configuration of DIC method setup.

As mentioned before, two of each variant of specimens were captured by DIC in tension and two in compression with focus on previous fiber-free area of first generation of specimens. Below is presented result as Z axis displacement, (direction of view of the DIC images) which proved before to be a reliable indicator of potentially problematic area. Captures of all specimens both in tension and in compression right before failure showed that there is no more problem at this area. Specimens SN_02 and SN_08 and tension specimens of SN_07 variant showed quite uniform displacement in Z axis as is shown on example of SN_02 tension specimen in Fig. 5a. On the other hand, the SN_07 specimens loaded in compression showed different result as they suffered sudden loss of stability of composite tube before failure of ILT joints. Example of DIC result of compression specimen SN_07 is shown in Fig. 5b. The last variant of specimens SN_09 was not subjected to DIC measurements.

3.2 AE method

There were two configurations of AE method based on previous experience which was given by some issues of AE sensors during experimental measurements. Sensors were always located on the wider area of tube surface as shown in Fig. 6. One of these configurations was used on each specimen except the SN_09 tension specimens:

- Four AE sensors divided by two on both sides of specimen and located 40 mm outside the center of tube. One upper located and one lower located (Fig. 6 – right side).
- Three AE sensors on one side of specimen located in the center of specimen and 40 mm outside the center of specimen tube, also one upper located and one lower located (Fig. 6 – left side).

The number of counts was evaluated from recorded data in dependence to the measured force. Examples of most common results could be seen in Fig. 7a section for SN_07 tension loading scenario and in Fig. 7b section for SN_07 compression loading scenario. The first one in Fig. 7a shows change in increase of counts which indicates increasing of local failures of specimen and might be used for some failure prediction. On the other hand, the second one in Fig. 7b does not show significant change in increase of counts from the first recorded. Computed Tomography (CT) analysis of future specimens is planned so the comparison of AE measuring with this analysis could be useful.

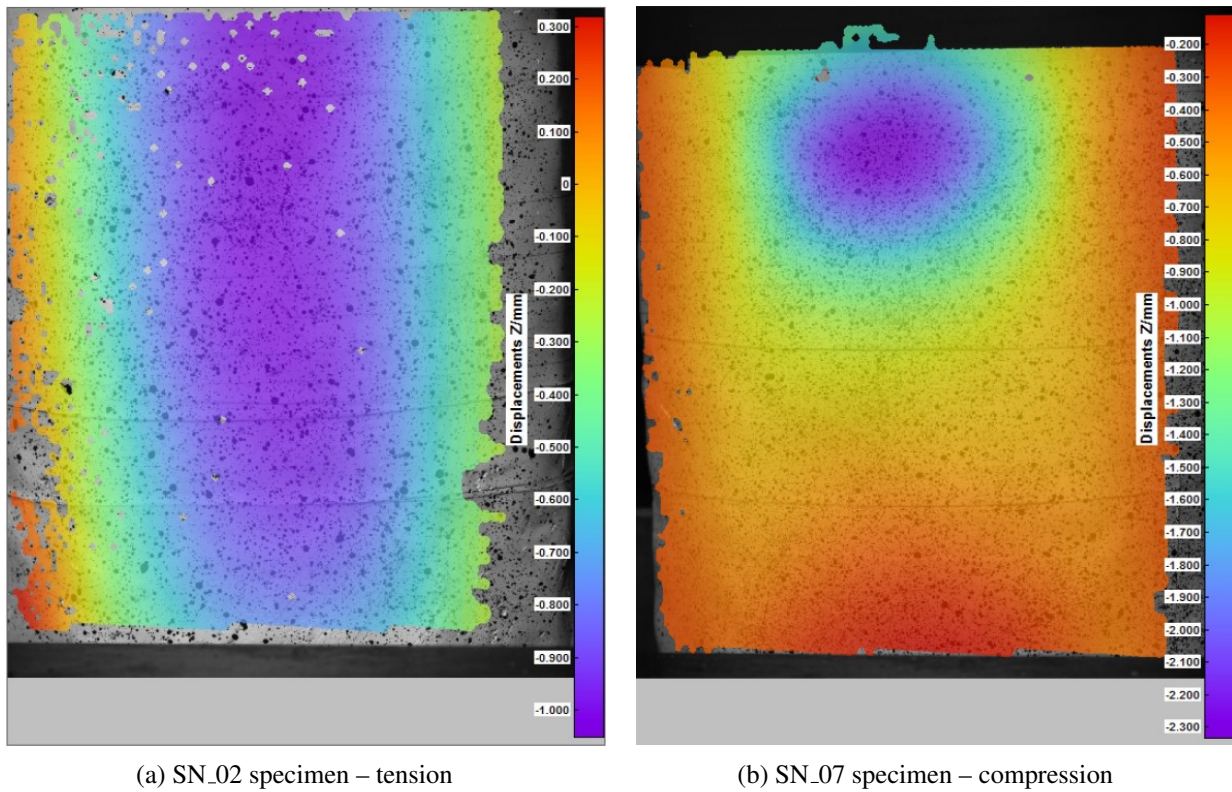


Fig. 5: Z axis direction displacement of chosen specimens measured by DIC method right before final failure.

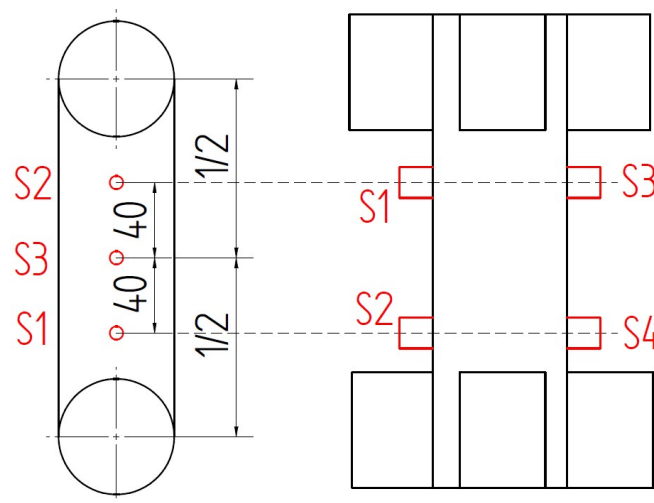


Fig. 6: Configuration of AE method setup.

3.3 Strain measurement

Due to the complexity of FEM analysis and the fact that the FE model was much more rigid than the measured data of displacement, the strain measurement was done on all specimens. Therefore 1-axis linear strain gauge was installed in the middle of narrower surface area of tube, oriented in the direction of applied loading as could be seen in Fig. 8.

Results of experimental measurements given as dependence between related force and normalized strain are shown in Fig. 9. Section of Fig. 9a is focused on tension loading scenario and section of Fig. 9b is focused on compression loading scenario. There could be seen that the differences of measured strains between specimen types are not much different. Still the SN_09 specimens seem to be slightly more rigid than the other types which is quite expected given the composition of these specimens. Based on measured experimental strain values the FE analysis was modified to contain strain gauges and the results were much closer to the measured ones than with comparison of displacements.

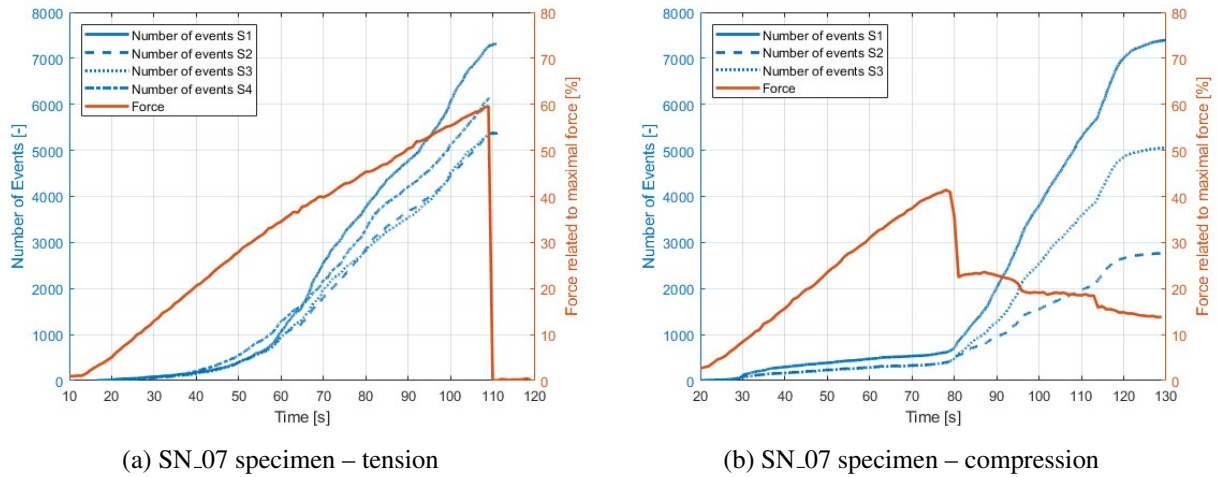


Fig. 7: Example of evaluated number of counts of AE method measuring compared with measured force presented on SN_07 specimens

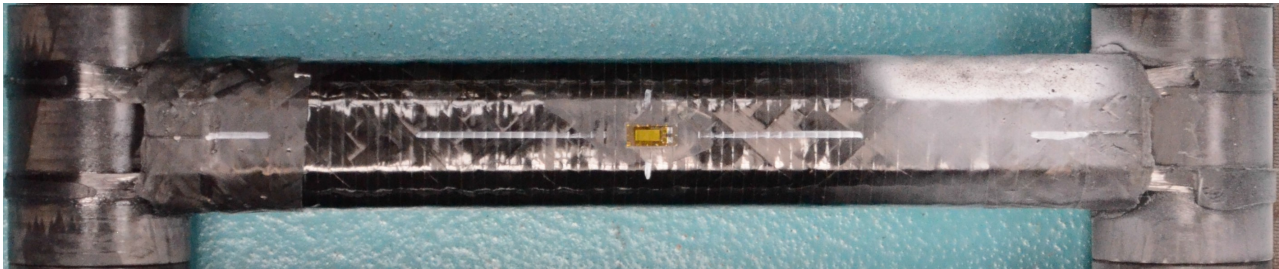


Fig. 8: One of measured specimens with installed strain gauge and sprayed grid used for DIC.

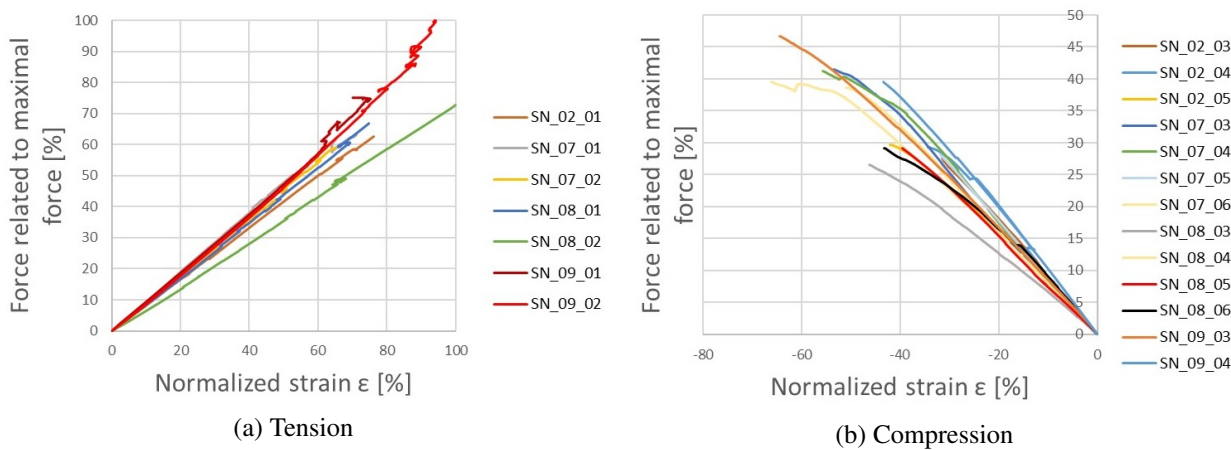


Fig. 9: Result of experimentally measured strains given as dependence between related force and normalized strain divided according to the loading scenario.

3.4 Video recording

Video recording was performed for all specimens. The camera position was given by the position of DIC setup since they couldn't take up the same side of the specimens. Therefore, camera was placed from side of loading machine taking the narrower area of tube with whole ILT joints with pins inside. This composition gives us an idea of behaviour and failure of specimens and shows us some possible problems. The first problematic behaviour observable by eye on the recordings was fact, that the non-isotropicity of composite specimens given by their composition and production process could affect the results. For example, one of specimen loaded in tension partially failed when one side of wound fibers of single ILT joint broke. Even so, the specimen lasted another almost 15 % of tension loading before complete failure. Some recordings of specimens showed that the movable part of loading machine visibly moved fast with the failure of specimen. Upon closer look, it was

observed that the specimen was rotated off-axis from the axis of loading. This phenomenon together with the difference in displacements between FE analysis and experimental measurements led to another measurement.

Based on the above observations, high resolution camera recording was prepared with markers on pins inside fixtures to compare measured displacement given by machine and displacement acquired by Edge Detection Method (EDM) and to detect possible problematic behaviour of machine during loading. Experiment was recorded by one camera as a 2D configuration for specimens SN_09 once in tension and compression. This measuring showed that during the compression loading of specimen the lower fixture (static one) most probably rotated. Also, we evaluated displacement of this measuring and the comparison between displacement recorded by machine and this method is show in Tab. 3. Although the displacement evaluated from this experiment is still containing some clearances for example between pins and ILT joints the result is much more rigid and thus closer to the FE analysis results.

Tab. 3: Comparison of displacement measured by loading machine and evaluated from EDM measurement.

Displacement of SN_09	Loading machine [mm]	EDM [mm]	Difference [%]
Tension	5.3	3.8	39
Compression	1.9	1.7	12

3.5 Overview of experimental results

Most of the partial results have already been shown in sections devoted to experimental methods. Measured dependence of displacement of loading machine on related force is given in Fig. 10. Section Fig. 10a deals with the tension loading scenario and could be seen that the SN_09 specimens are there slightly more rigid than the others. Also measured data of compression loading scenario in Fig. 10b are presented. The beginning of the signals represents the clearances between the pin and ILT joint which was different for different specimens. Comparison of average maximal forces achieved during experiments is shown in Tab. 4.

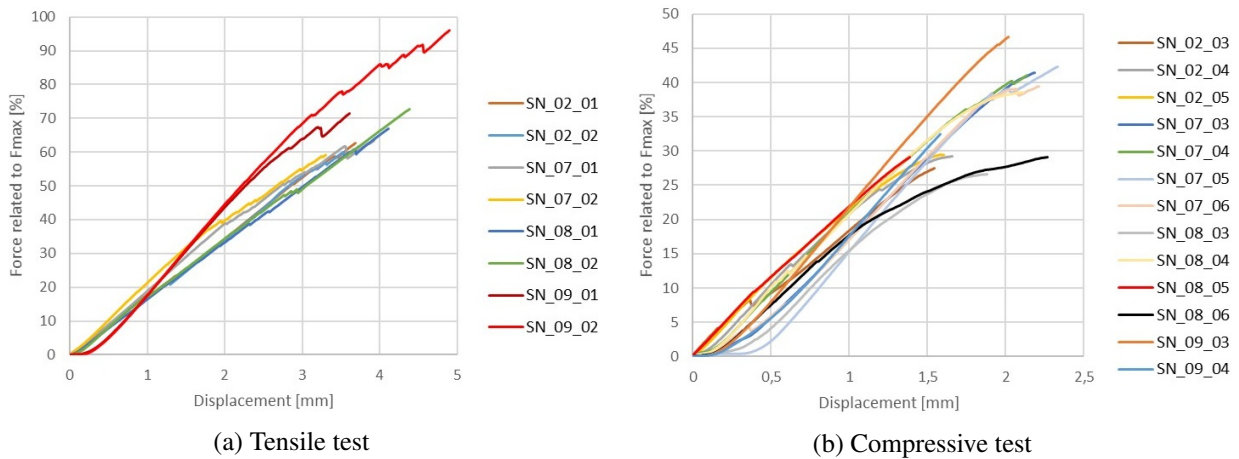


Fig. 10: Tensile test results given as dependence between related force and displacement.

Tab. 4: Experimental results given as average maximal force achieved during loading [%].

Specimen type	Tension	Compression
SN_02	62	29
SN_07	61	41
SN_08	70	31
SN_09	87	43

As could be seen from results, the influence of wrapping the fibers around tube of ILT joint proved to be

useful which could be seen on the SN_07 compression results. Also, the change in composition of specimens proved to be useful as could be seen on the SN_08 tension results. By combining of these findings with the technology demand was the SN_09 created and proved to be the most optimal variant. The sudden stability loss seen in compression of SN_07 specimens might be given by the fact that in all other experiments was the failed part the ILT joint and it happened by lower level of force. The SN_09 specimens did not show this type of failure.

4 Conclusion

Development of ILT joint according to the results of experimental measurements and monitoring was done. Experimental measurement was monitored by several different methods. DIC showed us that the previous fiber-free area was solved by the change of manufacturing technology and it pointed to a potential problem of sudden loss of stability of composite tubes by one variant of specimens. AE monitoring gave us dependence of counts on force during loading. Based on this result, it was decided to compare the measurement of AE with the CT of the next set of specimens. Strain measurement showed expected results in behaviour between variants of specimens. Video recording showed some potential problems of experimental setup and evaluation of additional special measurement by EDM method gave us more precise estimation of displacement. All mentioned results were important for making a reliable FE analysis model. The most suitable design appears to be SN_09 which was chosen for additional testing with different loading scenarios, such as bending and torque tests. Also, some specimens of this variant were tested in tension and compression again to extend the statistics and to do the mentioned comparison of CT results with AE monitoring which will be published separately.

Acknowledgement

This work has been supported by project No. SGS21/151/OHK2/3T/12 of the Grant Agency of the Czech Technical University in Prague and by project No. TJ02000252 of the Technological Agency of the Czech Republic.

References

- [1] A. Malá, et al., Finite element analysis of composite tubes with integrated loop connections, Proceedings of computational mechanics 2019 (2019) 114–116, <https://dspace5.zcu.cz/bitstream/11025/36298/1/Mal%C3%A1.pdf>.
- [2] A. Malá, et al., Analýza tuhosti a pevnosti vinutých trubek s integrovanými spoji, Mechanika kompozitních materiálů a konstrukcí 2020 - sborník (2020) 15–19, ISBN 978-80-01-06767-3.
- [3] B. Kropík, et al., Identification of MTB enduro bicycle frame beaviour, Book of full papers (2020) 252–262, https://ean.vsb.cz/files/Book_of_Full_Papers.pdf.
- [4] B. Kropík, et al., Detection and Monitoring of Failures in CFRP Specimens with Integrated Joints by Acoustic Emission Method, 27th Workshop of Applied Mechanics - Proceedings (2019) 20–23, ISBN 978-80-01-06680-5.